

CHAPTER III

APPLICATION OF SPECTRAL DISTRIBUTION THEORY USING WILDENTHAL'S SD INTERACTION

3.1. WILDENTHAL'S UNIVERSAL SD INTERACTION

The uncertainty that lies in the applications of SDM, comes mainly from the choice of the interaction Hamiltonian. In the past the predictions of SDM were compared^{1),2),3)} with the corresponding shell model results using different realistic interactions whenever they were available. However, except for the universal sd interaction of Wildenthal⁴⁾ the shell model calculations for other interactions were not performed throughout the sd shell. Also their predictions are not in very good agreement with experimental data. On the other hand the Wildenthal's universal sd interaction with fixed single particle energies and A-dependent two-body matrix elements, the dependence being $(18/A)^{0.3}$ to take into account the growing nuclear size, was extraordinarily successful in reproducing binding energies, spectra, spectroscopic factors, B(E2), B(M1) and B(GT) values to an unprecedented degree of accuracy throughout the sd shell. With this success, on one hand one can use the interaction to predict unknown properties like B(E4) values, study of neutron-rich sd shell nuclei like ^{24}O , ^{32}Mg , etc., and on the other hand, one can utilise this interaction to test general approximate theories/models, like spectral distribution theory, which have much wider applicability for all nuclei across the periodic table by comparing their prediction using universal sd interaction with the shell model results in the sd shell. Thus the

comparisons of the calculations performed with universal sd interaction provide new stringent tests of the SDM theory. In the following we give a brief account⁵⁾ of our investigation of binding energies, spherical orbit occupancies and smoothed spectra using SDM with the universal sd interaction and compare them with the shell model results and experimental data.

3.2 APPROXIMATE SMOOTHED FORMS FOR THE DENSITY OF STATES

We mentioned in chapter II that though the action of a central limit theorem (CLT) in large spectroscopic spaces produces for $\rho(E)$ an asymptotic Gaussian form, in actual applications one should be careful to take account of small departures from this asymptotic form and reconstruct $\rho(E)$ incorporating^{6),7)} these departures. A Gaussian probability function $\rho_G(x)$ is fully described by its first two moments, related to the centroid (ϵ_x) and the width (σ_x), while in general the $\rho(x)$ needs for its description, other shape parameters, expressible in terms of higher order central moments (μ_r) or cumulants (k_r) with $r > 2$. The lowest two shape parameters are the skewness ($\gamma_1 = \mu_3 / \sigma^3$) and the excess ($\gamma_2 = \mu_4 / \sigma^4 - 3$) and it is seen through detailed shell model calculations in fixed-JT spaces that the deviation of the shell model spectrum from the one using a corrected Gaussian density (with the 'skewness' and 'excess' corrections built in) is small and can be treated as fluctuations^{1),6)}. The departure from normality using non-zero values of γ_1 and γ_2 becomes increasingly significant for accurate predictions as x moves away from the centroid region i.e. in the tail regions of the distribution of x . It is shown⁷⁾ that typically, for values of $|\gamma_1|, |\gamma_2| \leq 0.3$, the corrected Gaussian form is adequate within

the region 3σ from the centroid. But when the dimensionalities of the scalar-m space or the scalar-mT spaces are large, the spectroscopically and experimentally interesting region is beyond the 3σ limit and one should resort to configuration partitioning of the space.

Two different types of methods are in use in SDM for the representation of the smoothed $\rho(E)$ given its first four moments or equivalently $(\epsilon, \sigma, \gamma_1, \gamma_2)$. In the Gram-Charlier and Edgeworth representations the density is expanded in a series in terms of derivatives of an asymptotic density. In the Cornish-Fisher method a transformation of variable is made such that the transformed variable has the asymptotic density and the variable itself can be chosen to have a series representation. We give the details of Gram-Charlier(GC), Edgeworth(EW) and Cornish-Fisher(CF) representations in Appendix B and in the next section, use the CF representations for the calculation of binding energy and excitation spectra as it has a larger domain of applicability compared to the GC and EW expansions⁷⁾.

3.3. EVALUATION OF BINDING ENERGIES, EXCITATION SPECTRA AND OCCUPANCIES

We define the smoothed distribution function corresponding to the density $\rho(\Gamma, E)$ as

$$F(\Gamma, E) = \frac{d(m, \Gamma)}{(2\Gamma+1)} \int_{-\infty}^E \rho(\Gamma, E') dE' \quad (3.3-1)$$

Then $F(\Gamma, \infty) = \frac{d(m, \Gamma)}{(2\Gamma+1)}$ - this asymptotic value of F is equal to the total number of eigenvalues of $H(m, \Gamma)$. It is then evident that the function $F(\Gamma, E)$ counts the number of distinct eigenvalues upto the energy E and is a monotonic function increasing by unity at each distinct eigenvalue of

$H(m, \Gamma)$. To evaluate the eigenvalue spectrum, we use, in actual computation $d(m, \Gamma) = d(m, T, T_Z)$ dimensionality and therefore define the smoothed distribution function as

$$F(E) = \sum_m \int \rho_{mT}(E') dE' = \sum_m \int_{-\infty}^E d(m, T, T_Z) \rho_{mT}(E') dE' \quad (3.3-2)$$

Using this distribution function the energy value of the i th excited level E_i can be found by inverting the equation

$$F(E_i) = g_i = \sum_{j=1}^{i-1} (2j+1) + \frac{1}{2} d_i \quad (3.3-3)$$

where $d_i = 2j_i + 1$ is the degeneracy of the i th level. The procedure described here is due to Ratcliff⁶⁾ and is represented pictorially in the fig.3.3-F1. One can use the Gaussian form or Gaussian with (γ_1, γ_2) corrections in equation(3.3-2) and solve numerically⁶⁾ the equation (3.3-3) to get the ground state binding energy and excitation spectrum.

The occupancy of a single particle orbit s is the expectation value of the number operator $n_s = [2j_s + 1] \left(A^{j_s} \times B^{j_s} \right)^0$ in the nuclear many-body energy eigenstate $|E\rangle$. Its expectation value ranges from 0 to the maximum of $(2j_s + 1)$. The well known French-MacFarlane sum rules⁸⁾ relate the weighted sums of the spectroscopic factors to the occupancies, both for stripping and pickup processes. Thus the experimental single nucleon transfer reaction strengths when summed over all observed final states give a lower limit to the occupancy. In SDM, the occupancies can be calculated using equation (2.2-8) for the average expectation value of an operator. This is given at energy E by

$$n^{\Gamma}(E) = \langle E | n^{\Gamma} | E \rangle \quad (3.3-4)$$

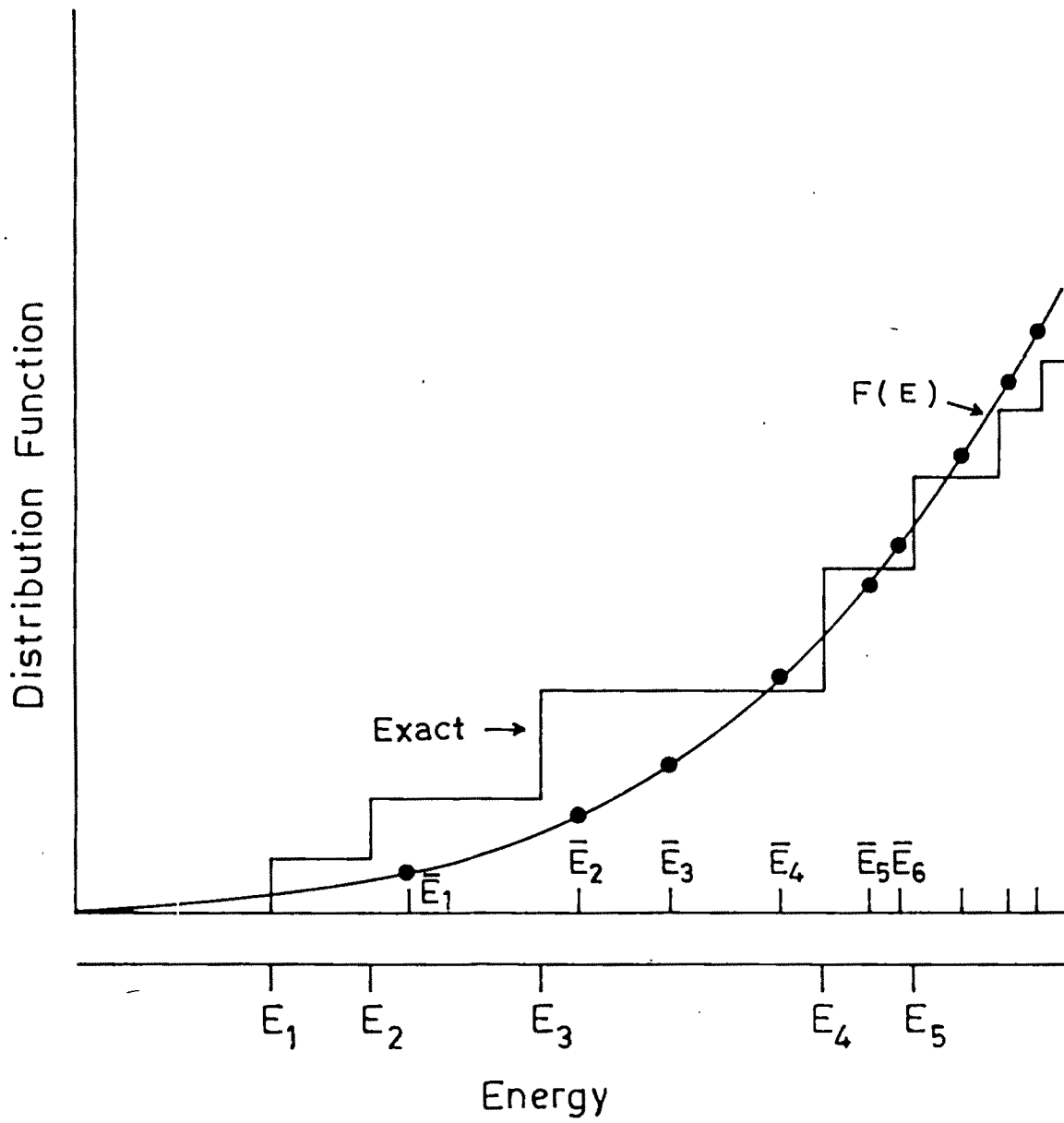


Figure 3.3-F1 : Illustration for the Ratcliff procedure. An exact distribution function represented by the staircase and its smoothed approximation (eq.(3.3-1)) along with the corresponding discrete spectra E_i and \bar{E}_i are shown.

$$\begin{aligned}
&= \sum_{\nu} \langle n^{\Gamma} P_{\nu}(H) \rangle^S P_{\nu}^S(E) \\
&\stackrel{\text{CLT}}{\simeq} \langle n^{\Gamma} \rangle + \langle n^{\Gamma} \tilde{H} \rangle^S \frac{(E - \langle H \rangle^S)}{\sigma^2(s)} \quad (3.3-5)
\end{aligned}$$

In equation(3.3-5) the CLT result retains terms with $\nu = 0$ and 1 only. We also note that $\tilde{H} = (H - \langle H \rangle^S)$ is the centred Hamiltonian and s denotes the relevant model space. The expressions for the occupancy upto the CLT limit has been evaluated in various model spaces. In the proton-neutron scalar space, $\mathcal{U}(N/2 : \text{proton}) + \mathcal{U}(N/2 : \text{neutron}) \subset \mathcal{U}(N)$, the proton occupancy in single particle orbit j , is given by⁹⁾

$$n_p^j(E) = \Omega^{-1} (2j+1) m_p \left\{ 1 + \frac{\Omega - m_p}{\Omega - 1} \zeta_j^P(m_p, m_n) / \sigma(m_p, m_n) \left(\frac{E - \langle H \rangle^S}{\sigma(m_p, m_n)} \right)^{m_p, m_n} \right\} \quad (3.3-6)$$

where $\Omega = N/2$ and $\zeta_j^P(m_p, m_n)$ is the traceless single-particle energy of a proton in orbit j , as modified by its interaction with the remaining $(m_p - 1)$ protons and m_n neutrons. For its expression in terms of the two-body matrix elements of H we refer to Potbhare and Pandya⁹⁾.

Similarly one can write the expression for occupancy in the scalar space [corresponding to the group $\mathcal{U}(N)$] :

$$n_s(E) = \langle n_s \rangle^{m, E} = \frac{N_s}{N} m + \frac{m(N-n)}{N(N-1)} \left\{ \tilde{\epsilon}_s + \frac{m-1}{N-2} \tilde{\lambda}_s \right\} \frac{\hat{E}}{\sigma(m)} \quad (3.3-7)$$

where $\hat{E} = (E - \langle H \rangle^S) / \sigma(m)$ and $\tilde{\epsilon}_s$ and $\tilde{\lambda}_s$ are traceless single-particle and single hole energies in the shell with degeneracy N and $\tilde{\lambda}_s$ is given⁹⁾ in terms of the matrix elements of the two-body part of H . It is to be noted that the occupancy calculated using the linear (in energy) theory in equation (3.3-7) above may sometimes turn out to be negative in the ground

state region, as the ground state is far below the centroid of the eigenvalue distribution and one needs further terms of the expansion to achieve better accuracy. However, the linear theory gives correct trends, the negative occupancy indicates a low or zero value of it.

On the other hand, if one partitions the model space into configurations i.e. $(\tilde{m}_p, \tilde{m}_n)$ or (\tilde{m}, T) corresponding to group

$$\left\{ \sum_r \left(U(2j_r+1)_p + U(2j_r+1)_n \right) \right\} \subset U(N) \text{ and } \left\{ \sum_r U(N_r/2) \times U_r(2) \right\} \subset U(N)$$

respectively, remarkable accuracy as well as simplicity results. As the number operator \tilde{n}_p^r or \tilde{n}_n^r are scalar operators under configuration partitioning, only $\nu = 0$ term in the polynomial expansion survives and leads to the result,

$$n_p^s(E) = \sum_{\tilde{m}_p, \tilde{m}_n} \frac{I_{\tilde{m}_p, \tilde{m}_n}^s(E)}{I_{\tilde{m}_p, \tilde{m}_n}(E)} m_p^s(\tilde{m}_p, \tilde{m}_n) \quad (3.3-8)$$

and for the configuration-T case, the occupancy of the s-th orbit at energy E is given by

$$n_s(E) = \sum_{\tilde{m}} \frac{I_{\tilde{m}}(E)}{I_{\tilde{m}T}(E)} m_s([\tilde{m}]) \quad (3.3-9)$$

TABLE 3.3-T1

Binding energies (BE) of nuclei in sd shell with universal sd interaction by spectral distribution methods along with experimental values and those by shell model. Column \bar{A} represents BE obtained using the simple Ratcliff procedure, column \bar{B} contains the BE corrected by integration up to an excited state, and column \bar{C} in addition, incorporates the (γ_1, γ_2) correction as given by equation (B-8) of Appendix B.

Nucleus		Expt. BE (in MeV)	BE by shell model with univ. sd interaction		BE by SDM (in MeV)	
A	Z		(in MeV)	\bar{A}	\bar{B}	\bar{C}
20	10	-40.48	-40.49	-40.04	-40.52	-38.51
21	10	-47.24	-47.20	-49.67	-47.63	-46.24
22	10	-57.60	-57.61	-62.88	-58.58	-56.50
23	11	-70.68	-70.67	-73.39	-73.39	-70.43
24	12	-87.10	-87.09	-93.14	-89.08	-84.91
25	12	-94.43	-94.39	-101.83	-97.96	-94.01
26	12	-105.53	-105.54	-116.58	-109.59	-104.72
27	13	-118.79	-118.82	-127.76	-124.26	-119.20
28	14	-135.70	-135.94	-145.43	-139.99	-134.10
29	14	-144.17	-144.35	-155.35	-149.06	-143.33
30	14	-154.78	-154.91	-166.07	-159.79	-154.77
31	15	-167.75	-167.89	-178.46	-172.09	-168.29
32	16	-182.62	-182.63	-191.57	-185.64	-182.30
33	16	-191.26	-191.14	-198.44	-193.71	-191.65
34	16	-202.68	-202.65	-209.56	-204.27	-202.46
35	17	-215.32	-215.43	-219.41	-215.86	-215.08
36	18	-230.41	-230.51	-232.91	-229.60	-229.04

In table 3.3-T1 we compare the binding energies of nuclei in the sd shell evaluated⁵⁾ by SDM using universal sd interaction with its shell model predictions as well as experimental values. From the column labeled \bar{A} of table 3.3-T1, we can see that the simple Ratcliff procedure of eq.(3.3-3) gives bad results, where in some cases binding energies deviate from experimental values by 10 MeV or more. The integration¹⁾ up to an excited state energy gives considerable improvement in the agreement (see column \bar{B}

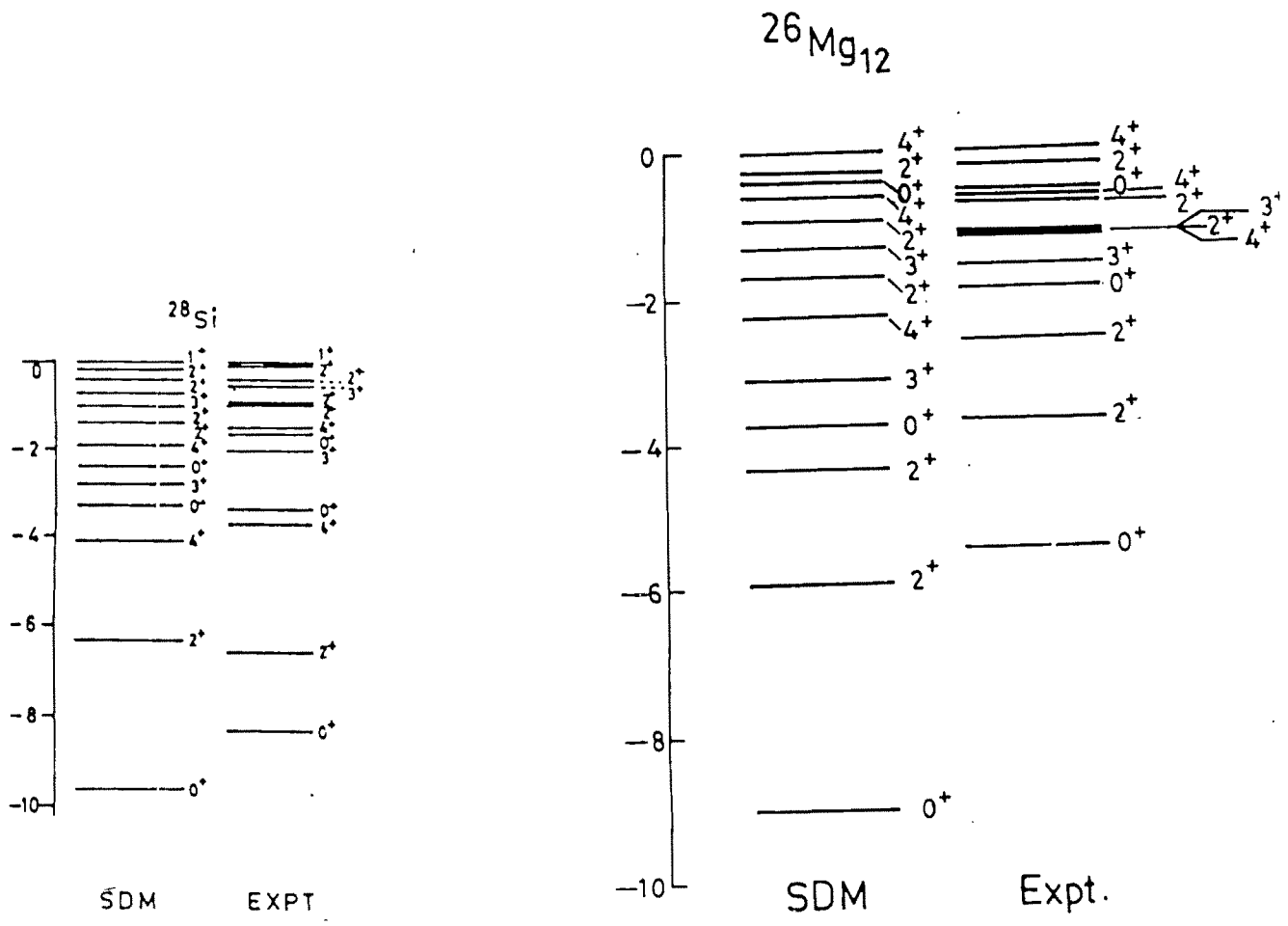


Figure 3.3-F2 : Energy spectra obtained by SDM using the universal sd interaction for ^{28}Si and ^{26}Mg are compared with experiment. In these comparisons the first 1^+ state for ^{28}Si and 3rd 4^+ state for ^{26}Mg are used as the reference states. Experimental data are from Endt and Van der Leun¹¹⁾.

of table 3.3-T1). We note that the experiments and compilations of von Egidy et al¹⁰⁾ are ideally suited for this type of calculations as they guarantee that in their data all levels up to and below a certain energy are all observed. For the present sd shell calculations we took the data from Endt and Van der Leun and other sources¹¹⁾. We also display in column \bar{C} of table 3.3-T1 the binding energies calculated by incorporating corrections due to non-zero (γ_1, γ_2) as given by eq.(B-8) of Appendix-B. Here we assume that the energies predicted by eq.(3.3-3) effectively arise from a single Gaussian, $\rho_{mT}(E)$, and further take for granted that $\gamma_1(mT) = \gamma_1(m)$ and $\gamma_2(mT) = \gamma_2(m)$; at present $\gamma_1(m)$ and $\gamma_2(m)$ are the easiest to calculate. Ideally one should evaluate the skewness and excess in (mT) spaces and construct $\rho_{mT}(E)$ using these values. We did not adopt this rather detailed procedure. However, our simple method of including the (γ_1, γ_2) corrections reproduces the experimental trends remarkably well throughout the sd shell. Almost all predicted values lie within 1 MeV of the experimental (or shell model) values, except for the three nuclei in the lower half of the shell, where the differences are 2.0, 2.2 and 1.6 MeV for ^{20}Ne , ^{24}Mg and ^{28}Si , respectively. Keeping in mind that the uncertainties due to fluctuation effects are about 1-2 MeV, the agreement can be considered to be quite satisfactory. We note here that the correction introduced due to nonzero skewness and excess replace the previous attempts to correct the binding energies by empirical terms proportional to $\left[\begin{smallmatrix} m \\ 2 \end{smallmatrix} \right]$ and $T(T+1)^{1)}$ in the lower and upper half of the sd-shell, respectively. The (γ_1, γ_2) values, for the universal sd interaction in $m=4, 8, 12, 16,$ and 20 particle space are $(0.00, -0.30), (0.01, -0.20), (0.00, -0.21), (-0.05, -0.23),$ and $(-0.15, -0.38),$

respectively. All the ground state energies before (γ_1, γ_2) corrections are lower than the experimental values, and the negative value of γ_2 pushes them up and brings them close to the data.

One can utilize the Ratcliff procedure in determining not only the ground state energy but in reproducing the low-lying excited state spectrum. In fig.3.3-F2 we compare two such spectra obtained by using the universal sd interaction with the experimental spectrum for ^{28}Si and ^{26}Mg . We see that the ^{28}Si spectrum is fairly well reproduced but for ^{26}Mg the agreement is not so good. In principle, matrix diagonalization coupled with statistical methods might be more appropriate for studying the low-lying spectra; however, so far one does not have a sensible prescription for doing that.

TABLE 3.3-T2

Ground state occupancies of $1d_{5/2}$, $2s_{1/2}$, and $1d_{3/2}$ orbits as predicted by shell model and by spectral distribution methods using the universal sd interaction.

Nucleus		Occupancies					
A	Z	By shell model			By SDM		
		$d_{5/2}$	$s_{1/2}$	$d_{3/2}$	$d_{5/2}$	$s_{1/2}$	$d_{3/2}$
21	10	3.496	0.998	0.507	4.306	0.543	0.151
22	10	4.575	0.813	0.612	5.222	0.607	0.171
23	11	5.316	0.912	0.772	5.960	0.727	0.314
24	12	5.980	0.894	1.124	6.793	0.805	0.402
25	12	7.173	0.805	1.022	7.408	1.017	0.575
26	12	8.018	0.909	1.074	8.149	1.192	0.659
27	13	8.894	1.023	1.082	8.811	1.335	0.853
28	14	9.246	1.408	1.346	9.557	1.482	0.961
29	14	10.106	1.679	1.214	9.943	1.768	1.289
30	14	10.472	1.892	1.635	10.418	2.020	1.561
31	15	10.838	2.422	1.741	10.767	2.285	1.952
32	16	10.842	2.836	2.322	11.143	2.580	2.277
33	16	11.233	3.314	2.454	11.325	2.796	2.879
34	16	11.371	3.409	3.220	11.644	3.033	3.302
35	17	11.477	3.535	3.988	11.743	3.285	3.973

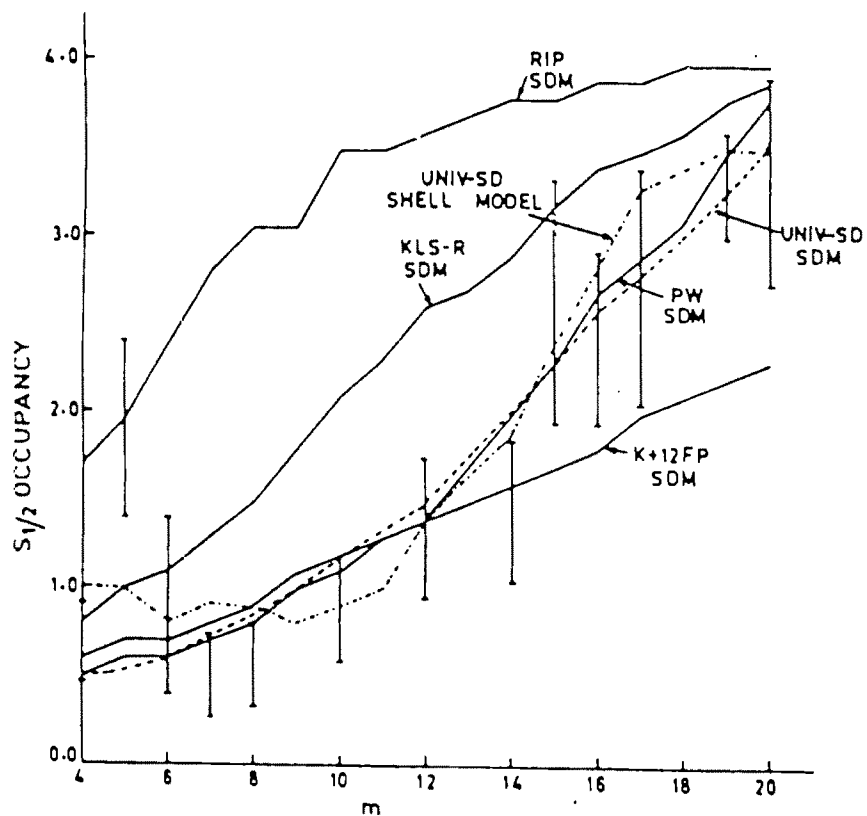


Figure 3.3-F3 : $s_{1/2}$ ground state occupancies by spectral distribution methods using universal sd as well as PW¹⁴⁾, RIP¹²⁾, KLS-R¹³⁾ and K+12FP¹²⁾ interactions compared with experimental values. The results for PW, K+12FP, RIP, and KLS-R interactions and experimental data are taken from Potbhare et al⁹⁾.

In Table 3.3-T2 we compare the predictions for the occupancies of the spherical orbits $1d_{5/2}$, $2s_{1/2}$ and $1d_{3/2}$ given by SDM with those by shell model using the universal sd interaction. Here we present results for nuclei with five or more particles (or holes) because for fewer particles the Gaussian approximation for $\rho_{mT}(E)$ is not a good one. In the calculations of occupancies we used binding energies as given by column \bar{B} of Table 3.3-T2 as we do not know $\gamma_1(\tilde{m}, T)$ and $\gamma_2(\tilde{m}, T)$ and column \bar{C} calculations are not exact. The SDM $d_{3/2}$ occupancy is low for lighter nuclei in the lower half of the sd shell, but the agreement becomes reasonably good near the middle and in the upper half. Comparisons of calculated occupancies for the $s_{1/2}$ orbit with experimental values obtained from stripping and pickup reactions were compared earlier⁹⁾ using different interactions. For example, the results with radial integral parametrized (RIP)¹²⁾, Kahana, Lee, and Scott (renormalized) KLS-R¹³⁾, Freedom and Wildenthal (PW)¹⁴⁾, and K+12FP¹²⁾ sd interaction are shown in fig.3.3-F3 along with the present calculations using universal sd interaction, and they are compared with the experimental $2s_{1/2}$ occupancies. The data clearly select not only the PW interaction, as pointed out by Potbhare and Pandya⁹⁾, but also the universal sd interaction. Potbhare and Tressler, also in their recent study¹⁵⁾ on the occupancy and single-nucleon strength function in the 2s1d shell using single-nucleon transfer sum rules have selected out of many available sd interactions only the PW and the universal sd interactions when they compared the $s_{1/2}$ occupancies and the occupancy dependent single particle energies with experimental values. In this work they also calculated the centroids and widths of the single nucleon transfer strength function. In this study we find that using universal sd interaction, the spectral distribution methods explain the ground state properties like binding energies and orbit

occupancies rather well, even though, a priori, one does not expect this. In particular we find that to locate energies of low-lying states, the deviations of the density of states from its asymptotic Gaussian form as measured through the nonzero skewness and excess supply the corrections in totally parameter-free form. We point out that the evaluations of the moments in fixed (J,T) spaces may improve the results even more. We also mention that the availability of shell model results on occupancies as a function of the excitation energy will allow one to make better tests of SDM. We conclude from our studies that future work, using SDM in the sd shell on excitation strengths and sum rules, should employ the Wildenthal's universal sd interaction.

REFERENCES FOR CHAPTER III

- 1). Chang F S, French J B and Wong S S M, Ann. Phys. (NY) 66 (1971) 137
- 2). Draayer J P, French J B and Wong S S M, Ann. Phys. (NY) 106 (1977) 472
- 3). Kar K, Nucl. Phys. A368 (1981) 285;
Chang F S and Zuker A P, Nucl. Phys. 198 (1972) 417;
Wong S S M and Loughheed G D, Nucl. Phys. 295 (1978) 289
- 4). Wildenthal B H, Prog. Part. Nucl. Phys. 11 (1984) 5
- 5). Sarkar S, Kar K and Kota V K B, Phys. Rev. C36 (1987) 2700
- 6). Ratcliff K F, Phys. Rev. C3 (1971) 117
- 7). Kota V K B, Potbhare V and Shenoy P, Phys. Rev. C34 (1986) 2330
- 8). French J B and MacFarlane M H, Nucl. Phys. 26 (1961) 168
- 9). Potbhare V and Pandya S P, Nucl. Phys. A256 (1976) 253;
Kota V K B and Potbhare V, Nucl. Phys. A331 (1979) 93
- 10). Von Egidy T, Behkami A N and Schimdt H H, Nucl. Phys. A454 (1986) 109
- 11). Endt P M and Van der Leun C, Nucl. Phys. A310 (1978) 1;
Lederer C M and Shirely V S (eds), Tables of Isotopes, 7th ed.
(Wiley, New York, 1978)
- 12). Halbert E C, McGrory J B, Wildenthal B H and Pandya S P,
Adv. Nucl. Phys. 4 (1971) 315
- 13). Kahana S, Lee H C and Scott C K, Phys. Rev. 185 (1969) 1378
- 14). Freedom B M and Wildenthal B H, Phys. Rev. C6 (1972) 1633
- 15). Potbhare V and Tressler N, Nucl. Phys. A530 (1991) 171